<category>Original

<title>Long-term fluid expulsion revealed by carbonate crusts and pockmarks connected to subsurface gas anomalies and palaeo-channels in the central North Sea

<author>Shyam Chand[1,2], Antoine Crémière[1,2], Aivo Lepland[1,2,3], Terje Thorsnes[1,2], Harald Brunstad[4], Daniel Stoddart[4]

[1]Geological Survey of Norway, Post Box 6315 Sluppen, 7491 Trondheim, Norway
[2]Centre for Arctic Gas Hydrate, Environment and Climate, University of Tromsø, 9037 Tromsø, Norway
[3]Institute of Geology, Tallinn University of Technology, 19086 Tallinn, Estonia
[4]Lundin Norway AS, Oslo, Norway

Present address, Daniel Stoddart: GeoEight AS, Bygdøy Alle 56C, 0265 Oslo, Norway

Corresponding author: Shyam Chand, e-mail: shyam.chand@ngu.no

Received: 30 August 2016 Accepted:

Abstract
Gas seepage through the seafloor into the water column is inferred based on acoustic mapping, video observations and geochemical analyses at multiple locations in the Viking Graben and Utsira High areas of the central North Sea. Flares in the Viking Graben occur both inside and along the periphery of a submarine melt water channel where pockmarks (up to 500 m in diameter) and methane-derived carbonate crusts are found on the seafloor, indicating focussing of fluid flow in the vicinity of the channel. The flares can be related to gas accumulations close to the seafloor as well as in Quaternary and deeper strata, observed as high-amplitude reflections on seismic data. Many palaeo channels, which act as accumulation zones, are observed in the subsurface of both Viking Graben and Utsira High areas. The deeper origin of gas is partially supported by results of isotope analyses of headspace gas collected from sediment samples of the Viking Graben, which show a mixed microbial/thermogenic origin whereas isotope data on free seeping gas in the Viking Graben indicate a predominantly microbial origin. Based on these lines of evidence, a structure

controlled fluid flow model is proposed whereby hydrocarbons migrate in limited amount from deep thermogenic reservoirs along faults, and these deep fluids are strongly diluted by microbial methane. Moreover, the existence of subsurface pockmarks at several stratigraphic levels indicates long-term fluid flow, interpreted to be caused by gas hydrate destabilisation and stress-related high overpressures.

<heading1>Introduction

Migration of pore fluids to the seafloor is common along oceanic margins, attributed to excess pore pressure resulting from various processes such as sediment loading/unloading (e.g. Hustoft et al. 2009), dissociation of gas hydrates (e.g. Chand et al. 2012), cap rock breach and faulting (e.g. León et al. 2014). One or a combination of these processes leads to morphological and geochemical/mineralogical expressions of fluid flow on the seafloor (Judd and Hovland 2009), which can be used for assessing the source of fluids and timing of their formation and perseverance. Active cold seeps are often linked to the formation of pockmarks (e.g. Hovland et al. 1984; Pau and Hammer 2013) and the presence of sub-seafloor hydrocarbon reservoirs (e.g. Milkov et al. 2003; Chand et al. 2012). Since the formation of pockmarks needs soft seafloor sediments which can be remobilised by fluid flow, cold seeps can be observed without pockmarks also (Brothers et al. 2011; Pau et al. 2014; Rise et al. 2015). Fluid flow processes in the subsurface are revealed as gas chimneys, wipe out zones and amplitude anomalies on seismic data, commonly coincident with observations of pockmarks, gas flares, bacterial mats and carbonate crusts on the seafloor (e.g. Cartwright et al. 2007; Løseth et al. 2009; Karstens and Berndt 2015; Landeghem et al. 2015). Hence, it has become a practice to use these proxies from both the surface and subsurface to assess past and present fluid flow, and decipher the maturity and nature of subsurface hydrocarbon reservoirs. The seafloor features give an indirect clue on how long the fluid flow has been active. For example, bacterial mats imply an active but short-term seepage (less than a couple of years) sufficient to enable a biological community to colonise the seep site (Judd and Hovland 2009). By contrast, carbonate crusts indicate a longer duration of seepage spanning hundreds to thousands of years (e.g. Bayon et al. 2009; Crémière et al. 2013; Berndt et al. 2014).

Gases originating from deeper reservoirs can be trapped in shallower reservoirs which poses a potential drilling hazard. This was the cause of massive gas blowouts in the central North Sea lasting over several decades, reported to have been the strongest gas seepage quantified to date (Schneider von Deimling et al. 2007; Leifer and Judd 2015). The contribution of methane to the atmosphere from cold seeps is also gaining importance due to their potential influence

on global climate change (Hartmann et al. 2013). It is estimated that marine methane emissions may contribute about 20 Tg year^{-1} to the global atmosphere methane budget (Etiope et al. 2008). Hence, it is important to map methane anomalies in sediment successions and reliably assess their formation and persistence within and outside offshore hydrocarbon provinces.

Fluid flow, shallow acoustic anomalies and geochemical characteristics of gases in different parts of the North Sea have been investigated in detail by many geophysical and geochemical studies inferring localised fluid flow models for specific areas (Rise et al. 1999; Mazzini et al. 2003; Fichler et al. 2005; Schroot et al. 2005; Hübscher and Borowski 2006; Hovland 2007; Andresen et al. 2008; von Deimling et al. 2011; Haavik and Landrø 2014; Karstens and Berndt 2015; Crémière et al. 2016). Numerous pockmarks were found in different parts of the North Sea (Hovland and Sommerville 1985; Rise et al. 1999; Hovland 2007; Gafeira 2012) that have been related to shallow gas availability and fluid migration pathways (Gafeira 2012). Palaeo seeps and carbonate structures were observed at Eocene level (Mazzini et al. 2003) and seafloor (Hovland et al. 1987; Crémière et al. 2016) indicating fluid seepage from deep towards the surface. Palaeo-iceberg plough marks concentrate shallow gas in the deep subsurface as well (Fichler et al. 2005; Haavik and Landrø 2014). A large number of seismic chimneys were reported from the Viking Graben (Karstens and Berndt 2015) which is proposed to have been initiated by mechanisms such as seal weakening, formation-wide overpressure and presence of free gas as essential prerequisites. Also evidence for fluid flow structures has been provided by mud diapirs and sand intrusions (Løseth et al. 2003).

Large amount of methane emission occurs from abandoned wells in the Central North Sea, attributed to be derived from shallow gas pockets penetrated by wells (Vielstädte et al. 2015). Isotope analyses of headspace gases from various locations in the North Sea suggest that the gases leaking are generally of microbial origin (Brekke et al. 1997), whereas gases collected at active seeps show a thermogenic origin (Hovland and Sommerville 1985). A recent study by Crémière et al. (2016) showed that the gas seepage happened over a long time period, albeit as distinct events. Stable hydrogen and carbon isotope compositions of methane in gas samples suggests mixing of microbial methane with a minor thermogenic methane (Crémière et al. 2016).

Based on all previous studies, a microbial methane dominated setting with minor thermogenic contribution is observed in the central North Sea. Along with the ambiguity in confirming the sources of microbial and thermogenic methane, the pathways of methane transit to the seafloor and control on ascend and timing are not resolved. The present study examines the

central North Sea subsurface fluid flow on a regional scale to understand the basin scale fluid flow pattern. Suspected structural and stratigraphic controls of fluid flow suggested in many earlier study areas of North Sea are critically evaluated using data from the Utsira High and the Viking Graben (Fig. 1). A combination of multibeam echosounder, high/low resolution seismic and geochemical data served to characterise fluid flow anomalies in the water column, seafloor and sub-seafloor providing a full picture of the fluid flow happening from subsurface to surface.

<heading1>Geological setting

The North Sea has a long structural and geological history. The most prominent structural changes occurred during the Caledonian orogeny (Silurian) with the formation of NE–SW oriented compressional structural elements superimposed on older Precambrian elements (Jordt et al. 1995; Nøttvedt et al. 1995). The faults from the Caledonian orogeny were reactivated during subsequent Variscan (late Carboniferous), Cimmerian (late Jurassic) and Alpine (mid Cainozoic) tectonic events (Isaksen and Tonstad 1989). In late Palaeozoic and early Triassic times, tensional forces resulted in the supercontinent break up and opening of the North Atlantic during the Tertiary, creating the Viking Graben. The N–S striking faults in the Horda platform area became reactivated during the Jurassic–Cretaceous, leading to further development of the Viking Graben (Nøttvedt et al. 1995; Gabrielsen et al. 2015). The Utsira High is an intrabasinal structural high between the Viking Graben and the Stord Basin (Fig. 1), formed during rifting (Gregersen et al. 1997).

Changes in sea level have been the main factors controlling sedimentary processes in the region (Isaksen and Tonstad 1989; Nøttvedt et al. 1995; Anell et al. 2012). A major phase of uplift and erosion during the early Cretaceous resulted in widespread regression which formed isolated sedimentary basins where deposition took place under dominantly anaerobic bottom conditions (Clausen et al. 2000; Isaksen 2004; Anell et al. 2010). Shales with high TOC contents deposited during the late Jurassic to early Cretaceous, including the Kimmeridge Clay, as well as the Mandal, Draupne and Tau formations represents the main source rocks of the North Sea (Gautier 2005). The main reservoir rocks consist of early and late Jurassic non-marine fluvial sediments of the Statfjord formation. Other reservoir rocks from pre-, syn- and post-rift times are rarer (Gautier 2005).

The North Sea seafloor morphology was carved under the influence of many glacial–interglacial cycles during the Quaternary, including three ice ages, the Elsterian, Saalian and Weichselian (Stoker et al. 1985; Cameron et al. 1987; Wingfield 1989; Sejrup et al. 1991;

Nygård et al. 2005). The most extensive glaciations of the North Sea Basin occurred between 200 and 450 ka (Sejrup et al. 1991). The conditions during the Quaternary varied between a present-day water depth of up to ~100 m, lowered sea level, glacial coverage with grounded ice (Chappell and Shackleton 1986; Fairbanks 1989) and even subaerial exposure (Sejrup et al. 1991). The Quaternary morphology is dominated by buried valleys, their origin being attributed to sub-glacial melt water transport incising the underlying Cainozoic strata during periods of glacial coverage (Huuse and Lykke-Andersen 2000; Huuse 2002; Fichler et al. 2005; Lonergan et al. 2006; Dowdeswell and Ottesen 2013; Ottesen et al. 2014). Sedimentation during the Quaternary in the central North Sea is characterized by rapid rates over short time intervals separated by long hiatuses (Sejrup et al. 1991; Haflidason et al. 1998; Lekens et al. 2009; Ottesen et al. 2014). Fine- to medium-grained sediments dominate the Pleistocene sequence. These sediments were suggested to have been re-deposited by rivers flowing northwards from the British Isles and the continent during periods of low sea level. The extreme lowstands of sea level are also indicated by river channels cutting into the sequence. After the retreat of the glaciers, the seafloor topography was smoothened by marine and glacio-marine sediments (Huuse and Lykke-Andersen 2000). Gently dipping Cainozoic and Mesozoic strata outcrop under the glacial sediments in the western and eastern parts of the North Sea, whereas Pliocene sediments cover the central part where the present study areas are located (Fig. 1). Several regional faults extend in a NE–SW direction (Fig. 1).
Pore pressure estimates from the North Sea indicate that high overpressure related to high stress resulted from deglaciation, flexure and compaction disequilibrium (Grollimund and Zoback 2000). High overpressure is inferred to be causing increased fluid flow towards the surface. Iceberg plough marks often act as accumulation and transport zones for gas (Haavik and Landrø 2014). Surface and subsurface expressions of gas seepage to the seabed are observed throughout the North Sea (e.g. Hovland and Sommerville 1985; Landrø and Strønen 2003; Schroot et al. 2005; Forsberg et al. 2007; Kilhams et al. 2011). Indeed, gas flares, carbonate crusts and near-surface gas anomalies have been reported throughout the region (e.g. Hovland and Sommerville 1985; Hovland et al. 1987; Brekke et al. 1997; Hovland 2007; Schneider von Deimling et al. 2011; Karstens and Berndt 2015), including recent findings for the present study areas in the central sector (e.g. Crémière et al. 2016).

<heading1>Materials and methods

<heading2>Bathymetry/backscatter

Multibeam echosounder (MBE) data were collected by the Norwegian Defence Research Establishment (FFI) using a Kongsberg EM710 echosounder during two cruises of 16–23 February 2013 and 5–14 March 2013 (Fig. 1). The EM710 system can also record water column data which can serve for the detection of active gas seeps.
The FlederMaus (FM) Midwater package was used to analyse water column data for evidence of gas anomalies. Seafloor reflection (i.e. backscatter) properties were derived in terms of the amplitude of the MBE data, providing indirect indications of sediment type/grain size and/or hardness of the top few decimetres below seafloor. MBE data for backscatter were processed by means of the FM Geocoder package.

<heading2>HUGIN AUV
The autonomous underwater vehicle (AUV) HUGIN was equipped with an EdgeTech 2200 high-resolution full spectrum chirp sub-bottom profiler (SBP) and a high-resolution interferometric synthetic aperture sonar (HISAS 1030). The SBP served to profile features of the immediate subsurface at very high resolution. The HUGIN was manoeuvred ~10 m above the seafloor at a constant speed, giving 50 cm horizontal resolution and a vertical resolution of less than 100 ms (~10 cm) with the SBP system. The HISAS 1030 provided a detailed bathymetry of the seabed, with a range-independent resolution of approximately 3×3 cm covering a distance of 200 m from both sides of the AUV at a speed of 2 m/s. The data were processed to generate high-resolution mosaics using Reflection software.

<heading2>Topas and 2D/3D seismics
The TOPAS parametric sub-bottom profiler was used to acoustically map the sediments in the uppermost part of the seabed. Layering can be clearly interpreted if the source signal can penetrate the seafloor sediments, giving a detailed stratigraphy of the uppermost few tens of metres. Topas data were collected along with multibeam echo sounder data during the main survey in February 2013.
Industry 2D and 3D seismic data from the DISKOS database were interpreted to infer structure, stratigraphy and subsurface anomalies using Petrel Software. Three main horizons, the Base Quaternary, Top Oligocene and Top Palaeocene, were interpreted using 2D seismic data based on a stratigraphic tie from the exploration wells 24/6-1, 24/6-2 and 24/6-4 (Fig. 1). Additionally, structural maps of the top Utsira (Top Miocene) and Base Pliocene interpreted using 2D/3D seismic and well data were available from Lundin Norge AS. The 3D seismic data served to examine the subsurface structure immediately below the seafloor using a Petrel

software variance volume attribute at 5×5 inline, crossline window and a smoothing factor of 25 samples. The variance attribute of Viking Graben data was taken at 240 ms TWT (two way travel time) and at 340 ms TWT for the Utsira High. The variance attribute gives an edge volume and hence is useful to map faults and channels.

<heading2>Sampling and geochemical analyses

One free gas sample was collected by ROV using a funnel attached to a gas cylinder in September 2013 (area a in Fig. 2a within the Alvheim channel (Crémière et al. 2016) in the Viking Graben area). Also, one headspace gas sample was collected from a push-core in the vicinity pockmark (a in Fig. 2a).

Gas aliquots were transferred into exetainers (0.1–1 ml) using a Gerstel MPS2 auto sampler and injected into a Agilent 7890 RGA GC equipped with Molsieve and Poraplot Q columns, a flame ionisation detector (FID) and thermal conductivity detector (TCD). Hydrocarbons were measured by FID, and H_2, CO_2, N_2 and O_2/Ar by TCD. The carbon isotopic composition of methane was determined by a Precon-IRMS system. Aliquots were sampled with a GCPal autosampler. CO_2, CO and water were removed on chemical traps. Hydrocarbons other than CH_4 and remaining traces of CO_2 were removed by cryotrapping. The methane was burnt to CO_2 and water in a 1,000 °C furnace over Cu/Ni/Pt. The water was removed by Nafion membrane separation. The Precon sample preparation system was connected to a Delta plus XP IRMS for $\delta^{13}C$ analysis. Repeated analyses of standards indicate that the reproducibility of $\delta^{13}C$ values is better than 1‰ PDB (2σ).

Thirty-four sediment samples from various depths of six push-cores (Fig. 2a) (up to 50 cm long) collected along the Alvheim channel were analysed for total organic carbon (TOC) content. Dried sediments were pulverized and decarbonated with 1M HCl. TOC content was measured on a LECO SC-632 analyzer, with an uncertainty better than 0.1% weight.

<heading1>Results

<heading2>Geophysical data

In all, 25 acoustic gas flares, up to 125 m high were detected in the Viking Graben during the study period, concentrated mainly along the western edge of the Alvheim channel (Fig. 3c). By contrast, 19 flares on the Utsira High occur randomly (Fig. 4a) and are only up to 70 m high (Fig. 3d).

The most prominent seafloor feature of the Viking Graben is the Alvheim channel. The water depth of the channel ranges from 113 to 168 m and the main channel is associated with

smaller and narrower channels to the west (Fig. 2a). Pockmarks are typically observed along the margins of the main channel but few also occur within the channel. Two large pockmarks within the channel coincide with flares (Fig. 3c). High backscatter is associated with the pockmarks and also with some mounds located along the channel margins (Fig. 2b).

The seafloor of the Utsira High is flat except for the E–W trending linear ridge in the northern part of the survey area with water depths ranging from 100 to 125 m (Fig. 4a). The ridge is criss-crossed by iceberg plough marks indicating limited post-glacial sedimentation (Fig. 4a). A few scattered depressions with nearby highs and high backscatter (Fig. 4) are most probably formed by anchoring of drilling rigs. High backscatter is observed along the E–W trending ridge and slightly higher backscatter in the SW sector (Fig. 4b). The latter is also earmarked by NW–SE and NE–SW oriented striations with high backscatter, probably indicating plough marks filled by post-glacial sediments. Three pipelines are observed as high backscatter linear features crossing the study area (Fig. 4b).

HISAS data reveal numerous carbonate crust locations along the Alvheim channel. Some locations in the northern part of the channel where two ~100 m high gas flares were recorded on 20th February 2013 were further investigated by ROV (Fig. 3a). The seabed at these locations is dominated by numerous furrows with scattered carbonate crusts (Fig. 3a, b). The seep system is presently diffuse since only a few bubbles were observed sporadically escaping from the seafloor on 2nd September 2013. Disseminated white patches of filamentous bacteria surrounding dark anoxic sediments suggest a relatively steady release of methane through the seafloor. HISAS data from the Utsira High show a muddy–sandy seafloor with no particular features. ROV inspection of the Utsira High flare locations did not reveal any carbonate crusts or bacterial mat patches. The seabed at the Utsira High is sandy with ripples indicating high current activity.

Topas data from a profile across one of the pockmarks in the Alvheim channel demonstrate active gas seepage with gas penetrating across the uppermost 5–10 ms stratigraphic layers (Fig. 5a). A nearby presently inactive pockmark, P1, must have been active formerly over a long time period, indicated by the presence of a coincident depression in subsurface stratigraphic layers (Fig. 5a). The northern part of the channel is filled with more than 20 m of stratified sediments which are lacking in the southern part of the channel (Fig. 5a, b). Layered sediments occurring in the channel pinch out towards the channel margin (Fig. 6b, c). The immediate subsurface shows distinct high-amplitude acoustic anomalies underlain by wipe out zones (Fig. 6a–c). The high-amplitude anomaly/wipe out zone boundary is concentrated at about 20 ms TWT (~15 m) below the seafloor but shallowing towards the

pockmark (Fig. 6a). A large wipe out zone is observed close to the shoulder of the channel where layered channel infill pinches out against older, acoustically chaotic sediments outside the channel (Fig. 6b, c). No wipe out zones or shallow gas anomalies occur outside of the channel (Fig. 6d). Disturbances due to faults extending from the Top Palaeocene to the Base Quaternary can be clearly seen (Fig. 7). High amplitude anomalies can be observed at the base of the channel fill sediments which also coincides with the Base Quaternary (Fig. 7a). The flare locations also have similar high amplitude anomalies at the Base Quaternary level (Fig. 7b).

The Alvheim channel extends further north, as observed on a 3D seismic variance attribute map of Quaternary sediments (240 ms TWT; Fig. 8a). Smaller subparallel palaeo channels occur west of the Alvheim channel. Palaeo-channels orientated E–W can be seen along the southern part of the Viking Graben area (Fig. 8a).

Gas-related blanking or wipe out zones in the subsurface were observed across four flare locations on the Utsira High (Figs. 5c, 9). Gas accumulation zones in the shallow subsurface are associated with high-amplitude anomalies followed by blanking or wipe outs (Fig. 9). A variance attribute map of the Utsira High indicates the presence of north–south oriented palaeo-channels within the Quaternary sediments (340 ms TWT) below the flare locations (Fig. 8b). On the Utsira High, the Base Quaternary is associated with numerous high-amplitude anomalies connected to the Top Oligocene and Top Palaeocene through a series of chimney-like structures with their bases starting at the Top Palaeocene (Fig. 10).

The interpretation of 2D industrial airgun seismic data shows that the Base Quaternary varies in depth from 200 ms TWT in the north-eastern part of the study area to 675 ms TWT along the southern part (Fig. 11a). The Top Oligocene varies in depth from 550 to 1,350 ms TWT, with the deepest part occurring along the Utsira High (Fig. 11b). The Top Oligocene is shallower at the Viking Graben compared to the Utsira high (Fig. 11b). The Top Palaeocene occurs as stratigraphic high at the Utsira High with the shallowest part occurring further to the east. In the Viking Graben, it is observed as a depression shallowing from the south towards the north where the Alvheim channel is located (Fig. 11c). The deepest part of the Top Palaeocene occurs along the southernmost part of the study area.

<heading2>Geochemical data

Free gas and sediment headspace gas from the Viking Graben are mainly composed of methane (>99.7%). Free gas shows a higher C_1/C_{2+} ratio of 1.6×10^6 with a more ^{13}C-depleted $\delta^{13}C\text{-}CH_4$ value of –71.7‰ VPDB whereas headspace gas has a lower C_1/C_{2+} ratio of 310 and

is less ^{13}C-depleted with a δ^{13}C-CH_4 value of –50.2‰ VPDB (Fig. 12a). The δ^{13}C-CH_4 versus C_1/C_{2+} plot indicates that the free gas sample from the Viking Graben falls in the microbial field whereas the headspace sample falls between the thermogenic and microbial field. The TOC content of sediments ranges between 0.2 and 0.65 wt%, with a distribution maximum at about 0.5 wt% (Fig. 12b).

<heading1>Discussion

<heading2>Source of methane

Shallow acoustic and geochemical gas anomalies from various parts of the North Sea from many studies suggested different fluid sources and flow mechanisms. In both the Viking Graben and the Utsira High, the chimney-like structures observed in the high-resolution seismic data at the shallow subsurface are connected to deep stratigraphic layers through faults and chimneys (Figs. 5, 6, 7, 9 and 10). The presence of gas at about 20 ms TWT below the seafloor and shallower wipe out zones at shallow gas pockets observed close to a pockmark suggests the movement of the gas front towards the leakage zone (Fig. 6a). The gas is focussed towards the Alvheim channel boundary where the recent sediment infill pinches out against older sediments outside the channel. A large seismic transparent zone occurring close to the shoulder of the channel indicates preferential lateral flow along layers towards the channel boundary (Fig. 6b, c). The high-amplitude reflections underlain by disturbances in seismic reflections show that the Base Quaternary level is a good accumulation zone at both the Viking Graben and the Utsira High close to flare locations (Figs. 7 and 10). The palaeo channels from previous glaciations are preferred locations for accumulation of gas and others fluids (Fig. 8). This is similar to structures reported from other areas of the North Sea where gas has been observed to be routed from deep sources (Brekke et al. 1997; Clayton et al. 1997).

Isotope data of free gas from the Alvheim channel indicate a main microbial source with a minor contribution from a deep thermogenic source (Fig. 12). Comparatively, the results from a previous study at the Utsira High (Vielstädte et al. 2015) show slightly different gas compositions with all samples within the microbial field but some trending towards the thermogenic field (Fig. 12a). The low TOC content observed in near-surface sediments suggests the unlikelihood of microbial gas production in these sediments. Instead, deeper organic-rich sediments are most likely the source for the generated microbial methane. Oligocene sediments with high TOC contents (>2%; Hordaland Group, North Sea well reports 24/6-1; NPD 2016) could be a major supplier of microbial methane as these sediments

are within the microbial methanogenesis window below 110 °C (Gold 1992; D'Hondt et al. 2004). Headspace gas analysis from well 24/6-1 also suggests a microbial window up to 1,400 m depth, which is deeper than the Oligocene sediments (NPD 2016). The carbon isotope results of the present study hence point to microbial gas generation within these high TOC sediments with a minor input from deeper thermogenic sources. The microbial methane is partly constrained at the top boundary of the Oligocene and shallower stratigraphic layers where high-amplitude anomalies are observed (Figs. 7 and 10). Shallow reservoir rocks above the Oligocene sediments (Gautier 2005) would promote accumulation as well as flow of deep microbial gases towards the locations of flares.

<heading2>Episodic fluid flow

The two study areas have similar water column and subsurface anomalies, even though the Utsira High lacks any observable fluid flow-related seafloor features such as pockmarks and carbonate crusts probably attributed to the coarse-grained nature of the sediments in the area. Topas data across one of the pockmarks with an active flare from the Viking Graben show incision into the top few metres of the sediment, indicating that these layers were removed during its formation (Fig. 5a). Dating results on methane-derived authigenic carbonate samples from the Viking Graben suggest that the seepage of microbial methane has persisted at least over the last 6,000 years (Alvheim channel; Crémière et al. 2016). The nearby inactive pockmark (P1) has subsurface depressions in many older stratigraphic layers, implying episodic fluid flow spanning a long time period (Fig. 5a). The 2D seismic data clearly indicate the fluid leakage from the Oligocene sediments, linking the gas flares to deeper sources (Figs. 7 and 10).

The long-term nature of fluid flow can be related to discharges from two possible sources. One source of gas is the melting of gas hydrates after the last deglaciation. Gas hydrates were stable during the last glacial maximum (LGM) in the study area, with methane hydrate stability zone thicknesses of at least 400 m (Fichler et al. 2005; Forsberg et al. 2007). The North Sea is currently too shallow for methane hydrate to be stable (Vogt et al. 1999; Fichler et al. 2005; Forsberg et al. 2007), and structure II hydrates cannot form due to the absence of higher-order hydrocarbon gases (pure methane down to 1,500 m in well 24/6-1; NPD 2016). Hence, the gas accumulated as gas hydrates during the LGM was potentially later released or even caused an overpressure scenario due to the expansion from solid gas hydrate to gas phase, resulting in the formation of pockmarks and continuous supply afterwards.

The other mechanism controlling fluid flow in the North Sea is stress accumulation due to glacial unloading (Grollimund and Zoback 2000). These overpressures can also open up fault pathways bringing the fluids to the surface, especially at structural highs since they are the loci of stress focussing during different time periods.

Therefore, a structure and stratigraphy-driven fluid flow model is suggested for the central North Sea as the regional model similar to most basins worldwide. The main addition to this model is the source driving the fluid flow which we propose as due to overpressures related to high stresses and changes in the hydrate stability zone. The methane is generated from microbial production within a zone extending as deep as Oligocene sediments. Deep-seated faults facilitate fluid flow towards the seafloor of the Viking Graben and the Utsira High, and palaeo-melt water channels within the Quaternary sediments act as good accumulation and focussing zones.

<heading1>Conclusions

1. Integration of seismic and water column data from the North Sea indicates that gas flares observed in the water column are partly connected to deeper sediments through faults and chimney structures extending up to the Oligocene strata.
2. Geochemical analyses of gas samples suggest a microbial source mixed with minor thermogenic components. Low TOC contents in near-surface sediments indicate a deeper microbial source for gas, inferred as Oligocene sediments with higher TOC contents.
3. The high-resolution seismic structure shows that gas from the deep strata accumulates in the shallow subsurface together with microbial methane generated in situ in the Quaternary and Tertiary sediments, and is released at specific locations in both the Viking Graben and the Utsira High.
4. Multiple levels of pockmarks indicate a long-term existence of fluid leakage facilitated by the accumulation and release of gas from a thick hydrate stability zone during the LGM, which destabilized after the retreat of glaciers and overpressures generated due to high stresses.

Acknowledgements

We thank Lundin Petroleum Norge AS for providing all support through the project, and the Norwegian Defence Research Establishment (FFI) in acquiring the data and samples used in the study. Also acknowledged are constructive assessments by M. Huuse and an anonymous reviewer on an earlier version of the article.

Conflict of interest: The authors declare that there is no conflict of interest with third parties.

References

Andresen KJ, Huuse M, Clausen O (2008) Morphology and distribution of Oligocene and Miocene pockmarks in the Danish North Sea–implications for bottom current activity and fluid migration. Basin Res 20:445–466

Anell I, Thybo H, Stratford W (2010) Relating Cenozoic North Sea sediments to topography in southern Norway: The interplay between tectonics and climate. Earth and Planet Sci Lett 300:19–32

Anell I, Thybo H, Rasmussen E (2012) A synthesis of Cenozoic sedimentation in the North Sea. Basin Res 24:154–179

Bayon G, Henderson GM, Bohn M (2009) U–Th stratigraphy of a cold seep carbonate crust. Chem Geol 260:47–56. doi:10.1016/j.chemgeo.2008.11.020

Berndt C, Feseker T, Treude T, Krastel S, Liebetrau V, niemann H, Bertics VJ, Dumke I, Dunnbier K, Ferre B, Graves C, Gross F, Hissmann K, Huhnerbach V, Krause S, Lieser K, Schauer J, Steinle L (2014) Temporal constraints on hydrate-controlled methane seepage off Svalbard. Science 343:284–287. doi: 10.1126/science.1246298

Brekke T, Lønne Ø, Ohm SE (1997) Light hydrocarbon gases in shallow sediments in the northern North Sea. Mar Geol 137:81–108

Brothers LL, Kelley JT, Belknap DF, Barnhardt WA, Andrews BD, Maynard ML (2011) More than a century of bathymetric observations and present-day shallow sediment characterization in Belfast Bay, Maine, USA: implications for pockmark field longevity. Geo-Mar Lett 31:237–248

Cameron T, Stoker M, Long D (1987) The history of Quaternary sedimentation in the UK sector of the North Sea Basin. J Geol Soc 144:43–58.

Cartwright J, Huuse M, Aplin A (2007) Seal bypass systems. AAPG Bull 91:1141–1166. doi: 10.1306/04090705181

Chand S, Thorsnes T, Rise L, Brunstad H, Stoddart D, Bøe R, Lågstad P, Svolsbru T (2012) Multiple episodes of fluid flow in the SW Barents Sea (Loppa High) evidenced by gas flares, pockmarks and gas hydrate accumulation. Earth Planet Sci Lett 331:305–314

Chappell J, Shackleton NJ (1986) Oxygen isotopes and sea level. Nature 324:137–140. doi: 10.1038/324137a0

Clausen OR, Nielsen OB, Huuse M, Michelsen O (2000) Geological indications for Palaeogene uplift in the eastern North Sea Basin. Global Planet Change 24:175–187

Clayton CJ, Hay SJ, Baylis SA, Dipper B (1997) Alteration of natural gas during leakage from a North Sea salt diapir field. Mar Geol 137:69–80. doi: 10.1016/S0025-3227(96)00080-1

Crémière A, Bayon G, Ponzevera E, Pierre C (2013) Paleo-environmental controls on cold seep carbonate authigenesis in the Sea of Marmara. Earth Planet Sci Lett 376:200–211. doi: 10.1016/j.epsl.2013.06.029

Crémière A, Lepland A, Chand S, Sahy D, Kirismae K, Bau M, Whitehouse MJ, Noble SR, Martma T, Thorsnes T, Brunstad H (2016) Fluid source and methane-1 related diagenetic processes recorded in cold seep carbonates from the Alvheim channel, central North Sea. Chem Geol doi: 10.1016/j.chemgeo.2016.03.019

D'Hondt S, Jørgensen BB, Miller DJ, Batzke A, Blake R, Cragg BA, Cypionka H, Dickens GR, Ferdelman T, Hinrichs KU, Holm NG, Mitterer R, Spivack A, Wang G, Bekins B, Engelen B, Ford K, Gettemy G, Rutherford SD, Sass H, Skilbeck CG, Aiello IW, Guerin G, House CH, Inagaki F, Meister P, Naehr T, Niitsuma S, Parkes RJ, Schippers A, Smith DC, Teske A, Wiegel J, Padilla CN, Acosta JLS (2004) Distributions of Microbial Activities in Deep Subseafloor Sediments. Science 306:2216–2221. doi: 10.1126/science.1101155

Dowdeswell J, Ottesen D (2013) Buried iceberg ploughmarks in the early Quaternary sediments of the central North Sea: a two-million year record of glacial influence from 3D seismic data. Mar Geol 344:1–9

Fairbanks RG (1989) A 17,000-year glacio-eustatic sea level record: influence of glacial melting rates on the Younger Dryas event and deep-ocean circulation. Nature 342:637–642

Fichler C, Henriksen S, Rueslaatten H, Hovland M (2005) North Sea Quaternary morphology from seismic and magnetic data: indications for gas hydrates during glaciation? Petrol Geosci 11:331–337

Forsberg C, Plank S, Tjelta T, Svanø G, Strout JM, Svensen H (2007) Formation of pockmarks in the Norwegian Channel. In: proc 6th Int Offshore Site Investigation and Geotechnics Conf, 11-13 September 2007. Society of Underwater Technology, London, pp 221–230

Gabrielsen RH, Fossen H, Faleide JI, Hurich CA (2015) Mega-scale Moho relief and the structure of the lithosphere on the eastern flank of the Viking Graben, offshore southwestern Norway. Tectonics 34:2014TC003778. doi: 10.1002/2014TC003778

Gafeira (2012) Semi-automated characterisation of seabed pockmarks in the central North Sea. Near Surf Geophys doi: 10.3997/1873-0604.2012018

Gautier DL (2005) Kimmeridgian Shales Total Petroleum System of the North Sea Graben Province. U S Geological Survey, Virginia

Gold T (1992) The deep, hot biosphere. Proc Nat Acad Sci 89:6045–6049

Gregersen U, Michelsen O, Sørensen JC (1997) Stratigraphy and facies distribution of the Utsira formation and the Pliocene sequences in the northern North Sea. Mar Petrol Geol 14:893–914. doi: 10.1016/S0264-8172(97)00036-6

Grollimund B, Zoback MD (2000) Post glacial lithospheric flexure and induced stresses and pore pressure changes in the northern North Sea. Tectonophysics 327:61–81

Haavik KE, Landrø M (2014) Iceberg ploughmarks illuminated by shallow gas in the central North Sea. Quat Sci Rev 103:34–50. doi: 10.1016/j.quascirev.2014.09.002

Haflidason H, King E, Sejrup H (1998) Late Weichselian and Holocene sediment fluxes of the northern North Sea Margin. Mar Geol 152:189–215

Hartmann D, Klein Tank A, Rusicucci M, Alexander LV, Bronnimann S, Charabi Y, Dentener FJ, Dlugokencky EJ, Easterling DR, Kaplan A, Soden BJ, Thorne PW, Wild M, Zhai PM (2013) Observations: atmosphere and surface. In: Climate Change 2013: The Physical Science Basis. Contribution of Working Group I to the Fifth Assessment Report of the Intergovernmental Panel on Climate Change, Cambridge University Press, Cambridge

Hovland M (2007) Discovery of prolific natural methane seeps at Gullfaks, northern North Sea. Geo-Mar Lett 27:197–201

Hovland M, Sommerville JH (1985) Characteristic of two natural gas seepages in the North Sea. Mar Pet Geol 2:319–326

Hovland M, Judd AG, King LH (1984) Characteristic features of pockmarks on the North Sea floor and Scotian Shelf. Sedimentology 31:471–480

Hovland M, Talbot MR, Qvale H, Olaussen S, Aasberg L (1987) Methane-related carbonate cements in pockmarks of the North Sea. J Sed Res 57:881–892

Hübscher C, Borowski C (2006) Seismic evidence for fluid escape from Mesozoic cuesta type topography in the Skagerrak. Mar Pet Geol 23:17–28

Hustoft S, Bünz S, Mienert J (2009) Three-dimensional seismic analysis of the morphology and spatial distribution of chimneys beneath the Nyegga pockmark field, offshore mid-Norway: 3D seismic analysis of the morphology and spatial distribution of chimneys. Basin Res 22:465–480. doi: 10.1111/j.1365-2117.2010.00486.x

Huuse M (2002) Late Cenozoic palaeogeography of the eastern North Sea Basin: climatic vs tectonic forcing of basin margin uplift and deltaic progradation. In: Bulletin of the Geological Society of Denmark. Aarhus Universitet, Copenhagen, pp 145–170

Huuse M, Lykke-Andersen H (2000) Over deepened Quaternary valleys in the eastern Danish North Sea: morphology and origin. Quat Sci Rev 19:1233–1253

Isaksen GH (2004) Central North Sea hydrocarbon systems: Generation, migration, entrapment, and thermal degradation of oil and gas. AAPG Bulletin 88:1545–1572

Isaksen D, Tonstad K (1989) A Revised Cretaceous and Tertiary Lithostratigraphic Nomenclature for the Norwegian North Sea. Norwegian Petroleum Directorate, Stavanger

Jordt H, Faleide JI, Bjørlykke K, Ibrahim MT (1995) Cenozoic sequence stratigraphy of the central and northern North Sea Basin: tectonic development, sediment distribution and provenance areas. Mar Pet Geol 12:845–879

Judd A, Hovland M (2009) Seabed fluid flow: the impact on geology, biology and the marine environment. Cambridge University Press, Cambridge

Karstens J, Berndt C (2015) Seismic chimneys in the Southern Viking Graben – Implications for palaeo fluid migration and overpressure evolution. Earth Planet Sci Lett 412:88–100. doi: 10.1016/j.epsl.2014.12.017

Kilhams B, McArthur A, Huuse M, Ita E, Hartley A (2011) Enigmatic large-scale furrows of Miocene to Pliocene age from the central North Sea: current-scoured pockmarks? Geo-Mar Lett 31:437–449

Landeghem KJJV, Niemann H, Steinle LI, O'Reilly SS, Huws DG, Croker PF (2015) Geological settings and seafloor morphodynamic evolution linked to methane seepage. Geo-Mar Lett 35:289–304

Landrø M, Strønen L (2003) 4D study of fluid effects on seismic data in the Gullfaks Field, North Sea. Geofluids 3:233–244

Leifer I, Judd A (2015) The UK22/4b blowout 20 years on: Investigations of continuing methane emissions from sub-seabed to the atmosphere in a North Sea context. Mar Pet Geol 68:706–717. doi: 10.1016/j.marpetgeo.2015.11.012

Lekens W, Haflidason H, Sejrup H, Nygard A, Richter T, Vogt P, Frederichs T (2009) Sedimentation history of the northern North Sea Margin during the last 150 ka. Quat Sci Rev 28:469–483

León R, Somoza L, Medialdea T, González FJ, Gimenez-Moreno CJ, Péréz-López R (2014) Pockmarks on either side of the Strait of Gibraltar: formation from overpressured shallow contourite gas reservoirs and internal wave action during the last glacial sea-level lowstand? Geo-Mar Lett 34:131–151

Lonergan L, Maidment SC, Collier JS (2006) Pleistocene subglacial tunnel valleys in the central North Sea basin: 3-D morphology and evolution. J Quat Sci 21:891–903

Løseth H, Gading M, Wensaas L (2009) Hydrocarbon leakage interpreted on seismic data. Mar Pet Geol 26:1304–1319. doi: 10.1016/j.marpetgeo.2008.09.008

Løseth H, Wensaas L, Arntsen B, Hovland M (2003) Gas and fluid injection triggering shallow mud mobilization in the Hordaland Group, North Sea. Geol Soc, London, Sp Pub 216:139–157. doi: 10.1144/GSL.SP.2003.216.01.10

Mazzini A, Duranti D, Jonk R, Parnell J, Cronin BT, Hurst A, Quine M (2003) Palaeo-carbonate seep structures above an oil reservoir, Gryphon Field, Tertiary, North Sea. Geo-Mar Lett 23:323–339

Milkov AV, Claypool GE, Lee Y-J, Xu W, Dickens GR, Borowski WS, ODP Leg 204 Scientific Party (2003) In situ methane concentrations at Hydrate Ridge, offshore Oregon: New constraints on the global gas hydrate inventory from an active margin. Geology 31:833–836. doi: 10.1130/G19689.1

Nøttvedt A, Gabrielsen R, Steel R (1995) Tectonostratigraphy and sedimentary architecture of rift basins, with reference to the northern North Sea. Mar Pet Geol 12:881–901

NPD (2016) Fact Pages, Norwegian Petroleum Directorate. http://www.npd.no/no/Tema/.

Nygård A, Sejrup HP, Haflidason H, Bryn P (2005) The glacial North Sea Fan, southern Norwegian Margin: architecture and evolution from the upper continental slope to the deep-sea basin. Mar Pet Geol 22:71–84

Ottesen D, Dowdeswell JA, Bugge T (2014) Morphology, sedimentary infill and depositional environments of the Early Quaternary North Sea Basin (56°–62° N). Mar Pet Geol 56:123–146

Pau M, Hammer Ø (2013) Sediment mapping and long-term monitoring of currents and sediment fluxes in pockmarks in the Oslofjord, Norway. Mar Geol 346:262–273. doi: 10.1016/j.margeo.2013.09.012

Pau M, Hammer Ø, Chand S (2014) Constraints on the dynamics of pockmarks in the SW Barents Sea: Evidence from gravity coring and high-resolution, shallow seismic profiles. Mar Geol 355:330–345. doi: 10.1016/j.margeo.2014.06.009

Rise L, Sættem J, Fanavoll S, Thorsnes T, Ottesen D, Bøe R (1999) Sea-bed pockmarks related to fluid migration from Mesozoic bedrock strata in the Skagerrak offshore Norway. Mar Pet Geol 16:619–631

Rise L, Bellec V, Chand S, Bøe R (2015) Pockmarks in the southwestern Barents Sea and Finnmark fjords. Norw J Geol 94:263–282

Schneider von Deimling J, Brockhoff J, Greinert J (2007) Flare imaging with multibeam systems: data processing for bubble detection at seeps. Geochem Geophys Geosyst 8:Q06004. doi: 10.1029/2007GC001577

Schneider von Deimling J, Rehder G, Greinert J, McGinnis DF, Boetius A, Linke P (2011) Quantification of seep-related methane gas emissions at Tommeliten, North Sea. Cont Shelf Res 31:867–878

Schroot BM, Klaver GT, Schüttenhelm RT (2005) Surface and subsurface expressions of gas seepage to the seabed—examples from the Southern North Sea. Mar Pet Geol 22:499–515

Sejrup HP, Aarseth I, Haflidason H (1991) The Quaternary succession in the northern North Sea. Mar Geol 101:103–111

Sigmond EMO (1992) Bedrock map of Norway and adjacent ocean areas, scale 1:3,000,000. Geological Survey of Norway, Trondheim

Stoker MS, Long D, Fyfe JA (1985) The Quaternary succession in the central North Sea. Newslett Strat 14:119–128

Vielstädte L, Karstens J, Haeckel M, Schmidt M, Linke P, Reimann S, Liebetrau V, McGinnis DF, Wallmann K (2015) Quantification of methane emissions at abandoned gas wells in the Central North Sea. Mar Pet Geol 68:848–860

Vogt P, Gardner J, Crane K (1999) The Norwegian–Barents–Svalbard (NBS) continental margin: introducing a natural laboratory of mass wasting, hydrates, and ascent of sediment, pore water, and methane. Geo-Mar Lett 19:2–21

Wingfield R (1989) Glacial incisions indicating Middle and Upper PIeistocene ice limits off Britain. Terra Nova 1:538–548.

Fig. 1 Locations of study areas off southern Norway (*inset*) covered by multibeam bathymetry (*black polygons*) shown on the regional bathymetry of that North Sea sector, together with the locations of faults (*dark grey lines*; NPD 2016), 24/6 wells (*yellow dots*), hydrocarbon discoveries (*orange polygons*; NPD 2016), 3D seismics (*red polygons*), sub-crop formation boundaries (*yellow dashed lines*; Sigmond 1992) and 2D seismics (*green lines*: *a* Fig. 7a, *b* Fig. 7b, *c* Fig. 10a, *d* Fig. 10b)

Fig. 2 a Bathymetry of the Viking Graben (extracted partly from Crémière et al. 2016), with locations of flares recorded on February and March, 2013 (*red squares*), carbonate crusts (*yellow dots*), push cores (*green triangles*), SBP lines (*a–d* Fig. 6a to d respectively) and Topas line (Fig. 5a, b). **b** Backscatter of the Viking Graben

Fig. 3 Seafloor observations: **a** Viking Graben: drop stones, carbonate crusts and muddy sediments; **b** Viking Graben: small holes which may represent gas escape features or burrows; **c** two flares in the Viking Graben (shaded relief bathymetry, bubble size exaggerated; for locations, see Fig. 2a); **d** flares on the Utsira High (shaded relief bathymetry, bubble size exaggerated; locations in Fig. 4a)

Fig. 4 a Multibeam bathymetry and **b** backscatter of the Utsira High. Also shown are the locations of flares recorded on February and March, 2013 (*red squares*), SBP lines (*a* Fig. 9a, *b* Fig. 9b) and Topas line (Fig. 5c)

Fig. 5 Topas lines **a** across large pockmarks in the northern part of the Alvheim channel; **b** southern part of the Alvheim channel; **c** across flares on the Utsira High (cf. locations of a and b in Fig. 2a and c in Fig. 4a)

Fig. 6 a–**c** SBP seismic lines in the Alvheim channel showing the build-up of gas fronts and chimney structures **a** across a pockmark, **b** across the side of a pockmark and starting from the shoulder of the channel, **c** up to the middle of the Alvheim channel and starting from the shoulder. **d** SBP seismic line westwards of the shoulder across a flare showing few gas-related anomalies, indicating that the gas mainly comes from the Alvheim channel (for locations of SBP lines, see a to d respectively in Fig. 2a). Also reported are the locations of carbonate crusts and gas flares

Fig. 7 a W–E 2D seismic line from the Viking Graben showing Base Quaternary, Top Oligocene and Top Palaeocene surfaces, as well as faults (*dotted lines*). **b** Neighbouring NW–SE 2D seismic line (for locations, see a and b respectively in Fig. 1)

Fig. 8 a Variance time slice at 240 ms TWT along the Viking Graben showing the subsurface structure of the Alvheim channel and nearby palaeo-channels. **b** Variance time slice at 340 ms TWT on the Utsira High showing many subsurface channels. *White dotted lines* MBB data, *blue dots* exploration wells

Fig. 9 SBP seismic lines on the Utsira High **a** across a flare and pipe line, **b** across a flare showing subsurface gas accumulations and chimney structures (for locations, see a and b respectively in Fig. 4a)

Fig. 10 a NW–SE 2D seismic line showing Base Quaternary, Top Oligocene and Top Palaeocene as well as faults (*dotted lines*) on the Utsira High. **b** Neighbouring N–S 2D seismic line (for locations, see c and d respectively in Fig. 1)

Fig. 11 Regional maps of **a** Base Quaternary, **b** Top Oligocene and **c** Top Palaeocene derived from 2D seismic data. *Black polygons* Locations of detailed study areas with multibeam bathymetry data, *red lines* faults

Fig. 12 a Carbon isotope of methane vs. hydrocarbon molecular composition (Bernard plot) for the Viking Graben based on the present and previous (Hovland et al. 1987) studies, Utsira High (Vielstädte et al. 2015) and Tommeliten areas (Hovland and Sommerville 1985), and. **b** TOC content (weight %) of sediment in the Viking Graben (n=34)

Figures

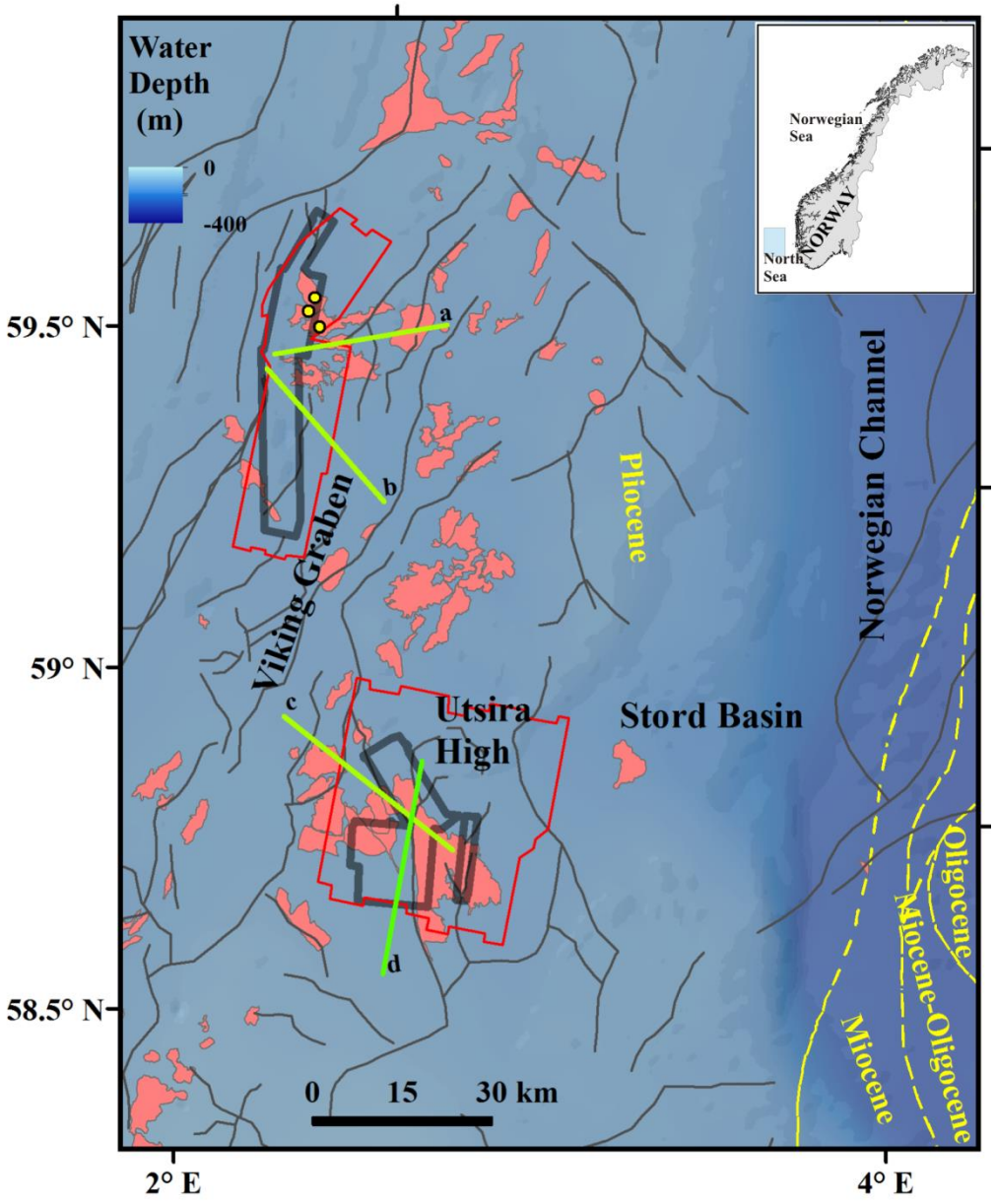

Figure 1.

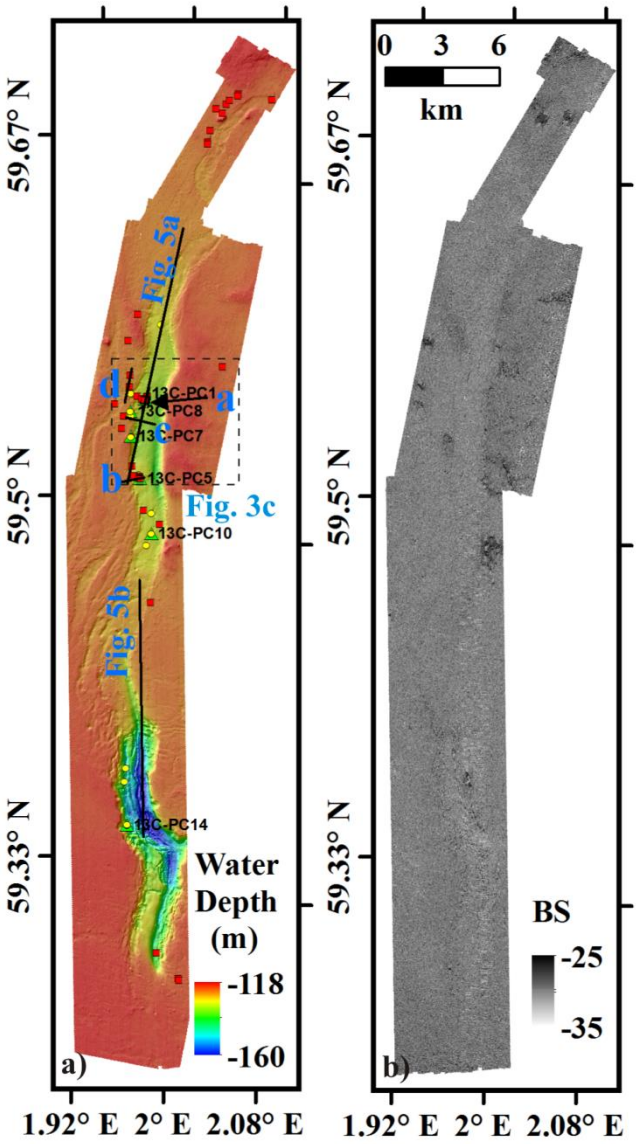

Figure 2.

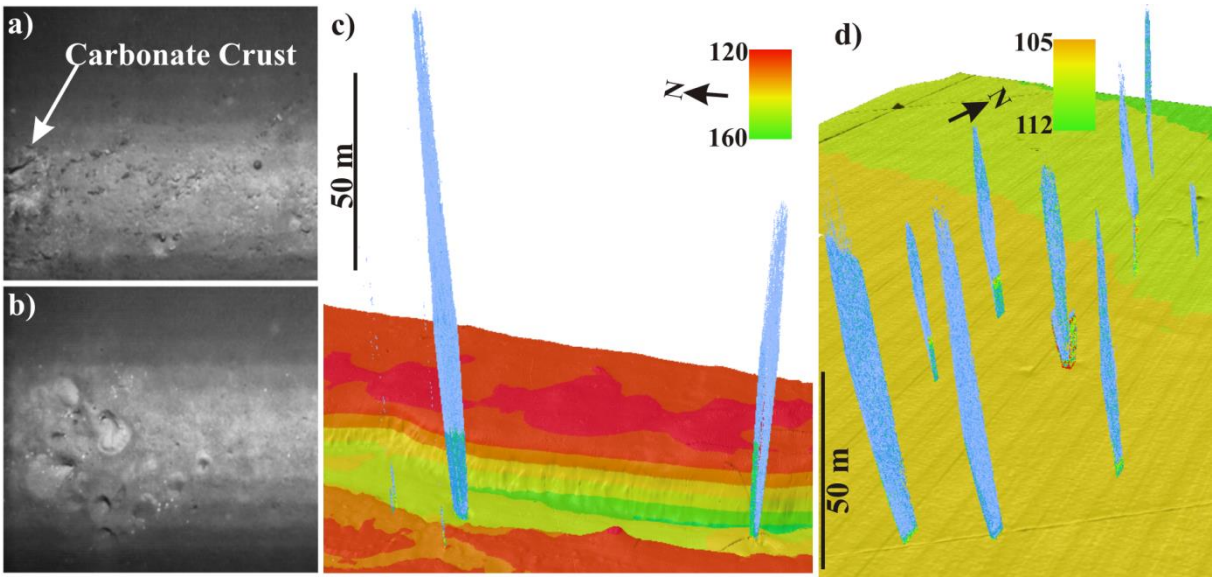

Figure 3.

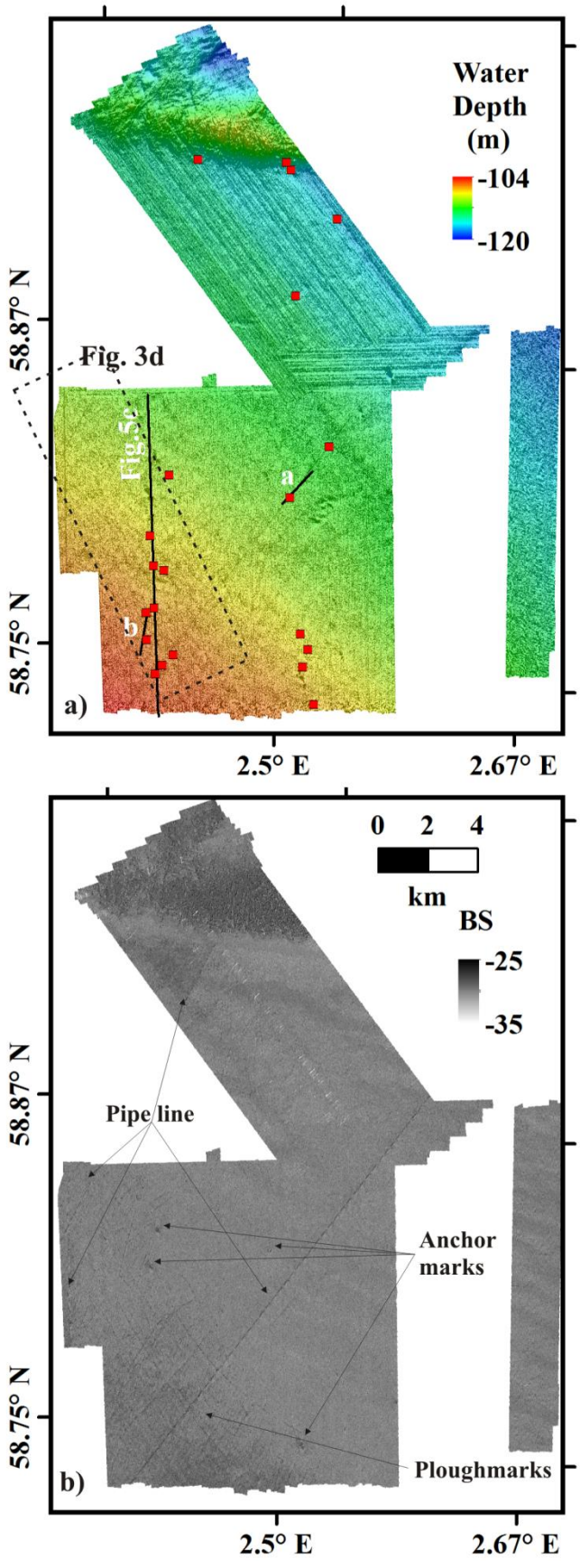
Water
Depth
(m)
-104
-120
Fig. 3d
Fig. 5c
a
b
a)
58.87° N
58.75° N
2.5° E
2.67° E
0 2 4
km
BS
-25
-35
Pipe line
Anchor
marks
Ploughmarks
b)
58.87° N
58.75° N
2.5° E
2.67° E

Figure 4.

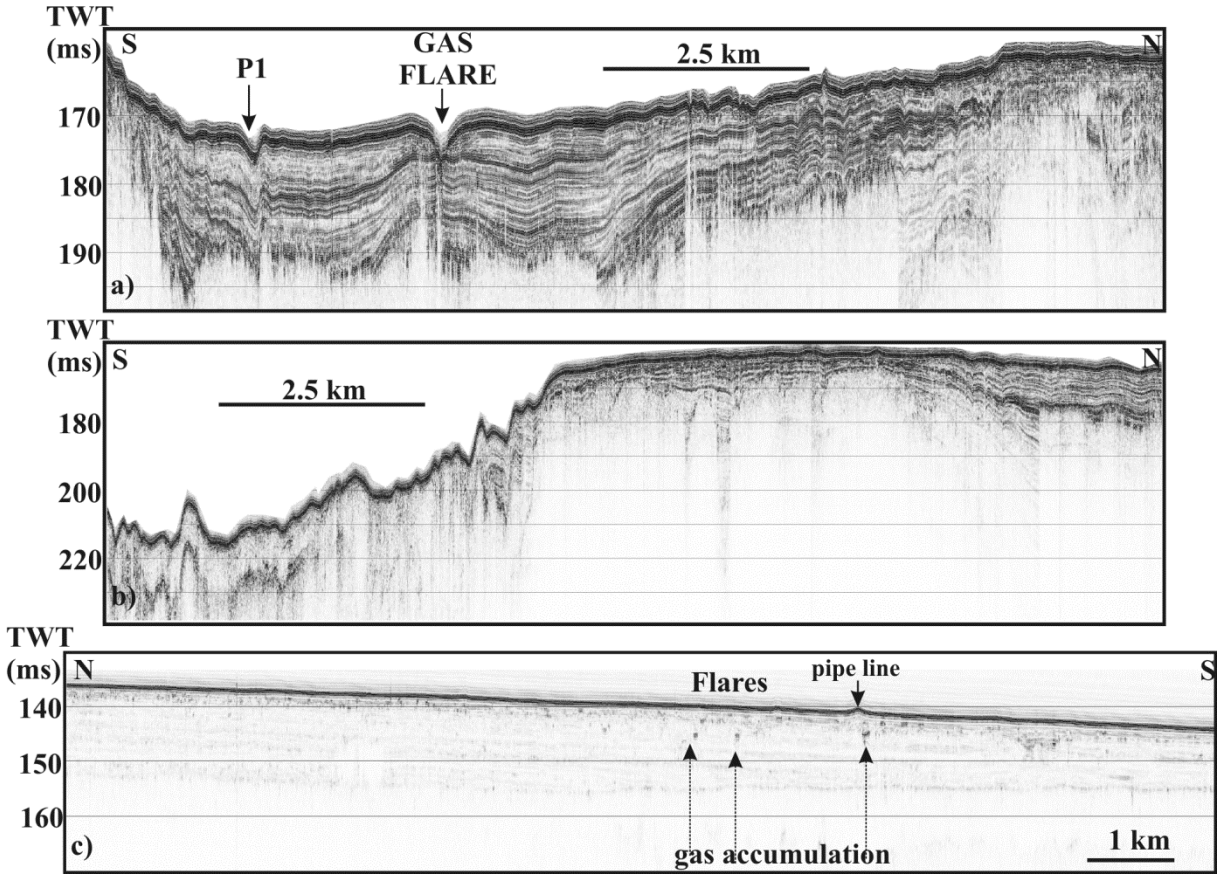
TWT
(ms)
S
P1
GAS
FLARE
2.5 km
N
170
180
190
a)
TWT
(ms)
S
2.5 km
N
180
200
220
b)
TWT
(ms)
N
Flares
pipe line
S
140
150
160
c)
gas accumulation
1 km
Figure 5.

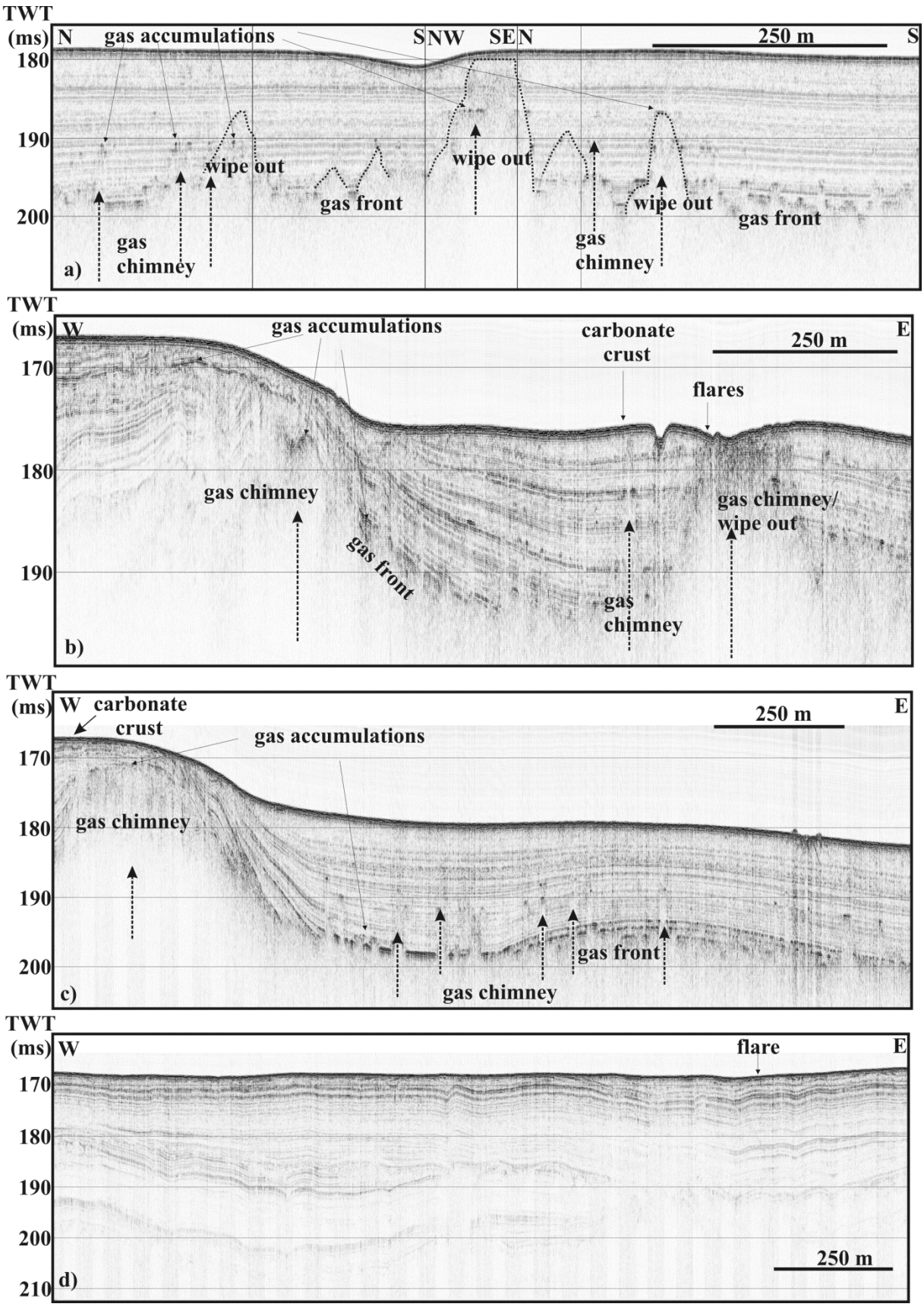
TWT
(ms)
N
gas accumulations
SNW
SEN
250 m
S
180
190
200
wipe out
wipe out
gas front
wipe out
gas front
gas chimney
gas chimney
a)
TWT
(ms)
W
gas accumulations
carbonate crust
250 m
E
170
180
190
flares
gas chimney
gas front
gas chimney/ wipe out
gas chimney
b)
TWT
(ms)
W
carbonate crust
gas accumulations
250 m
E
170
180
190
200
gas chimney
gas front
gas chimney
c)
TWT
(ms)
W
flare
E
170
180
190
200
210
250 m
d)

Figure 6

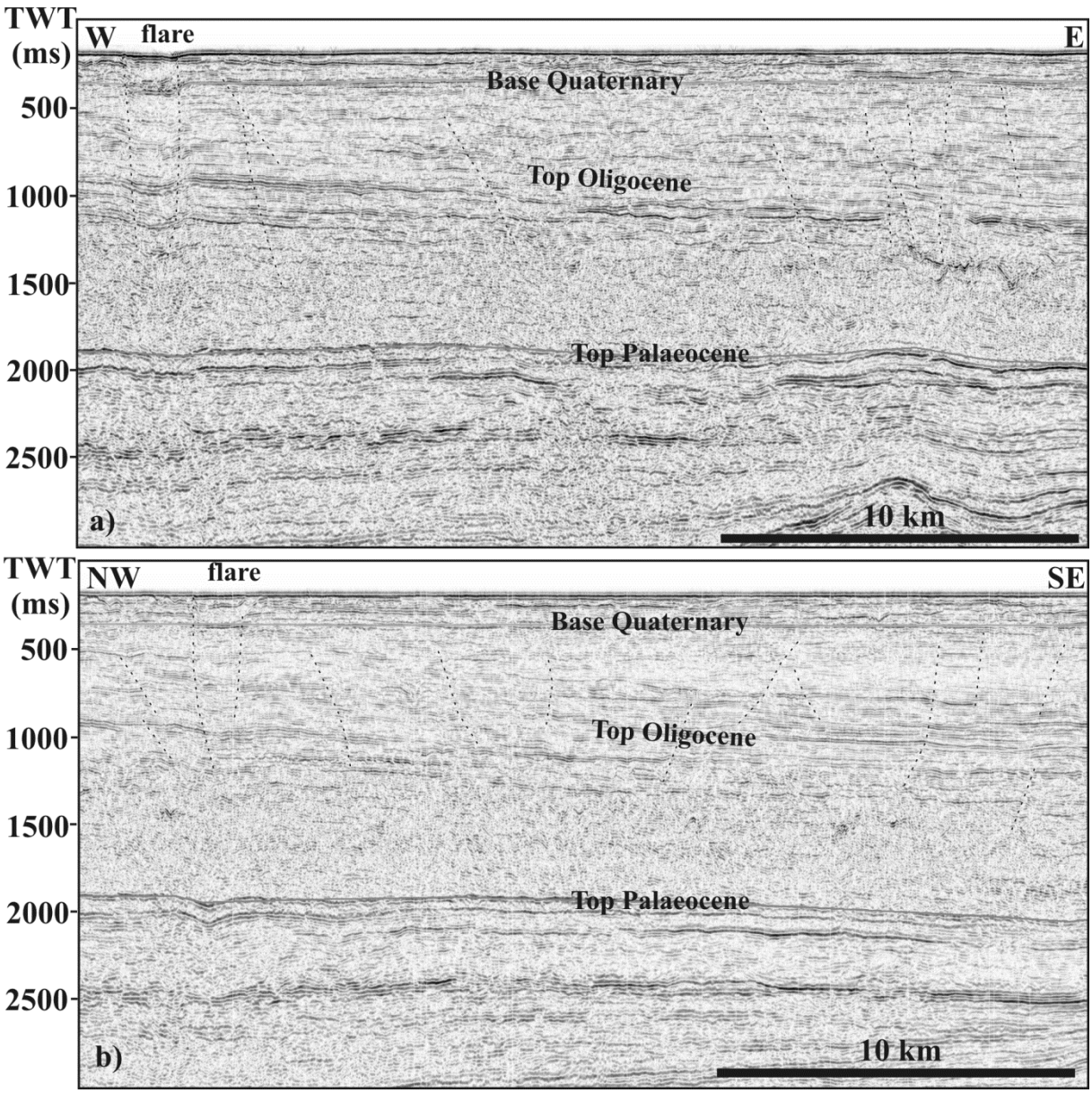
TWT
(ms)
W
flare
E
Base Quaternary
Top Oligocene
Top Palaeocene
500
1000
1500
2000
2500
a)
10 km
TWT
(ms)
NW
flare
SE
Base Quaternary
Top Oligocene
Top Palaeocene
500
1000
1500
2000
2500
b)
10 km

Figure 7.

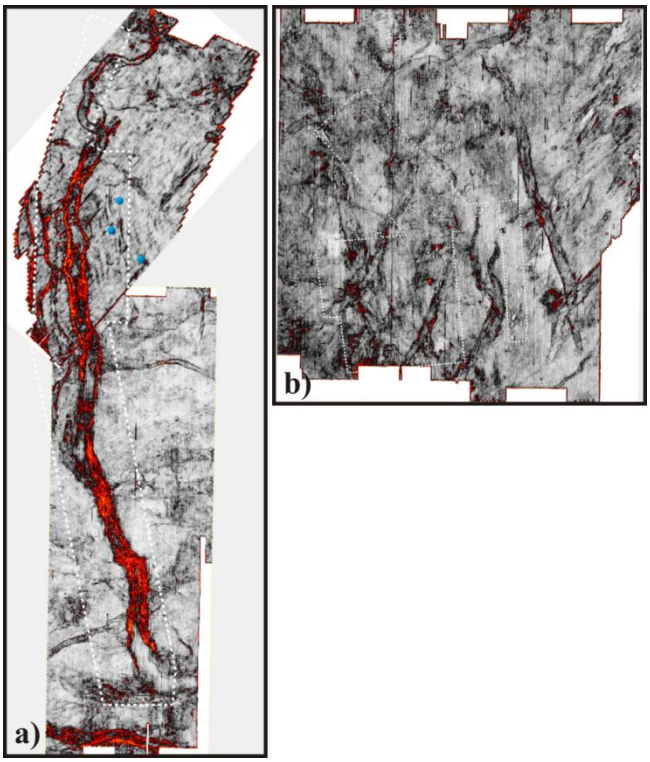

Figure 8

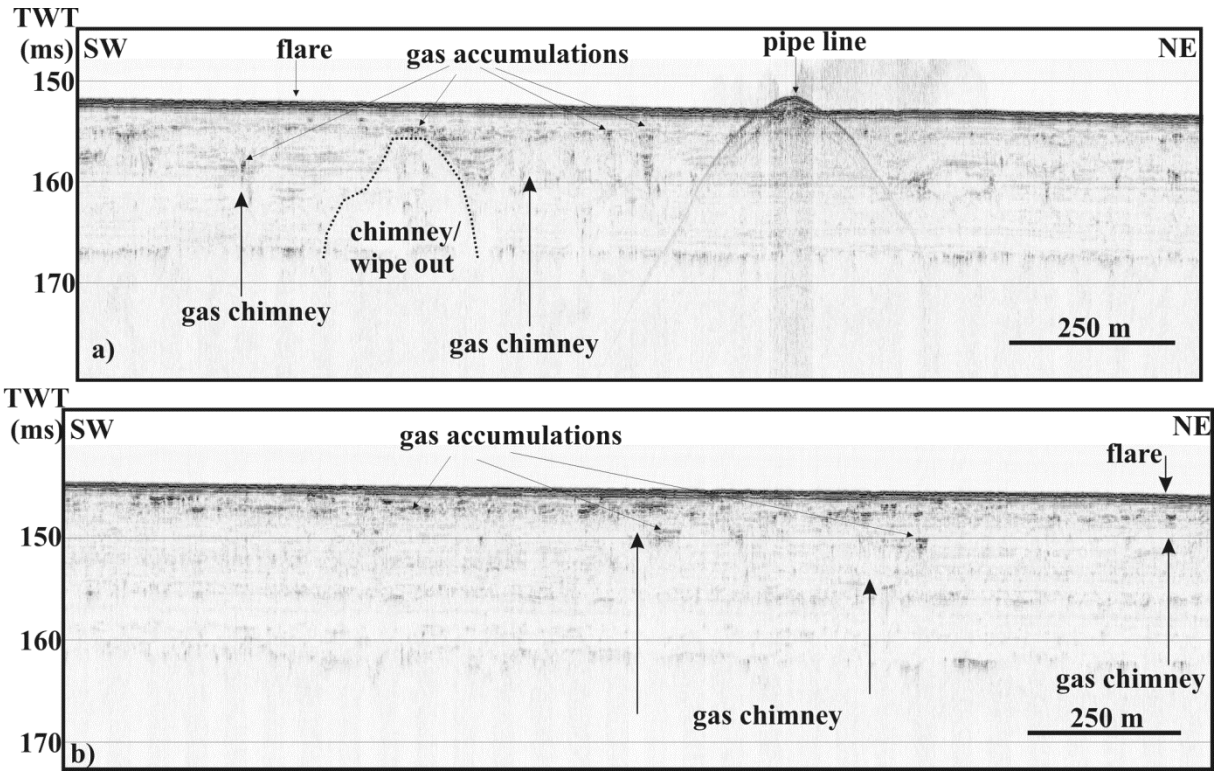
TWT
(ms)
SW
flare
gas accumulations
pipe line
NE
150
160
170
chimney/
wipe out
gas chimney
gas chimney
250 m
a)
TWT
(ms)
SW
gas accumulations
NE
flare
150
160
170
gas chimney
gas chimney
250 m
b)

Figure 9.

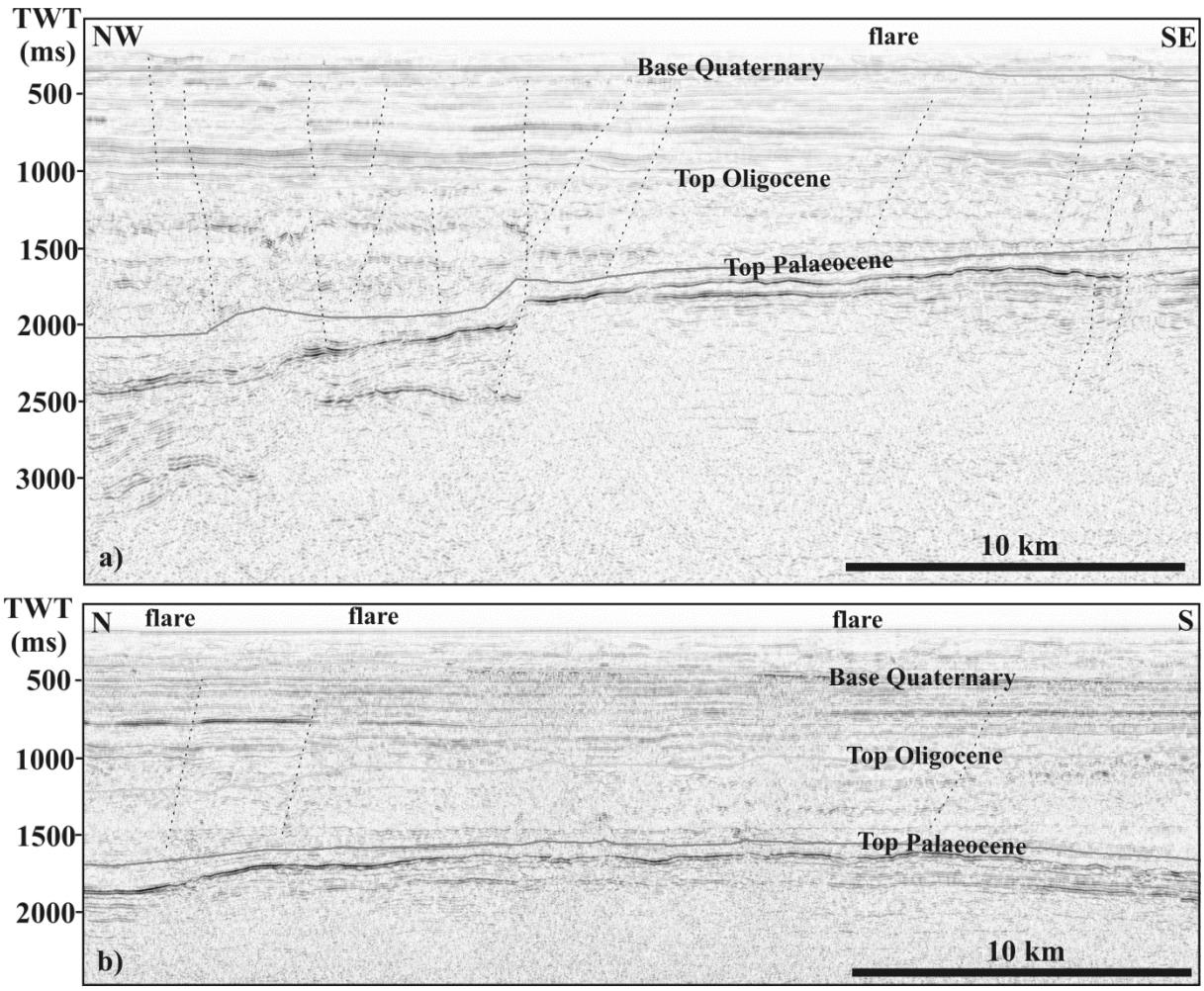
TWT
(ms)
NW
flare
SE
Base Quaternary
500
1000
Top Oligocene
1500
Top Palaeocene
2000
2500
3000
a)
10 km
TWT
(ms)
N
flare
flare
flare
S
500
Base Quaternary
1000
Top Oligocene
1500
Top Palaeocene
2000
b)
10 km

Figure 10.

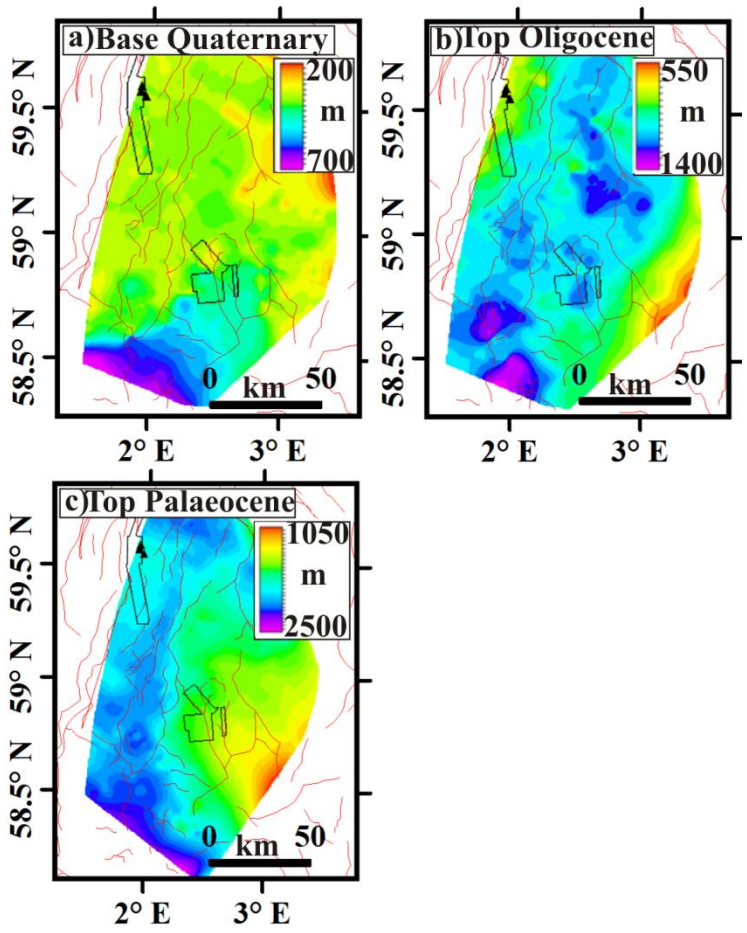
a)Base Quaternary
200
m
700
b)Top Oligocene
550
m
1400
c)Top Palaeocene
1050
m
2500
59.5° N
59° N
58.5° N
2° E
3° E
0 km 50

Figure 11

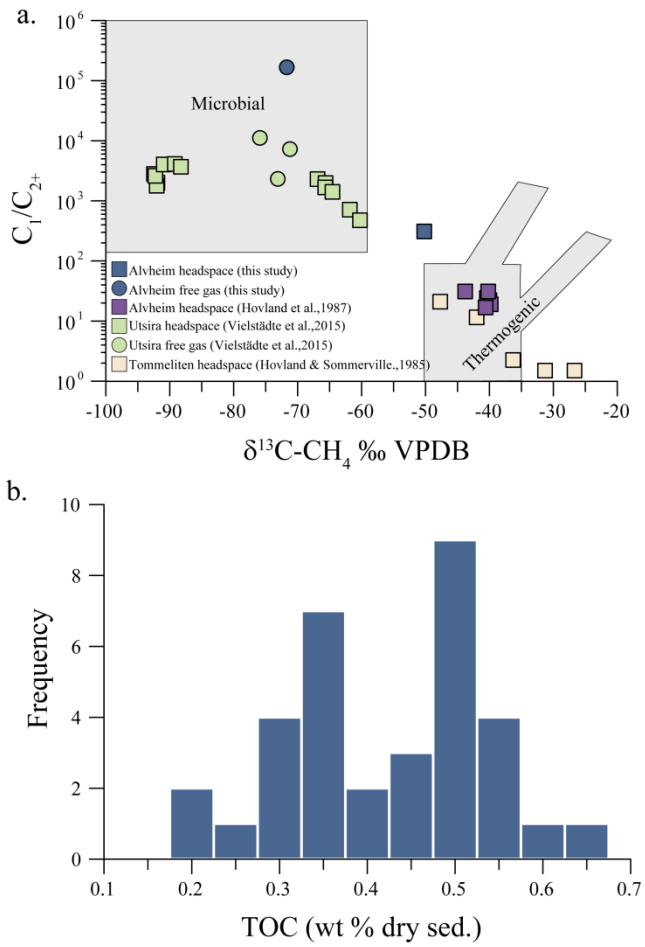
a.
Microbial
Thermogenic
Alvheim headspace (this study)
Alvheim free gas (this study)
Alvheim headspace (Hovland et al.,1987)
Utsira headspace (Vielstädte et al.,2015)
Utsira free gas (Vielstädte et al.,2015)
Tommeliten headspace (Hovland & Sommerville.,1985)
C1/C2+
δ13C-CH4 ‰ VPDB
b.
Frequency
TOC (wt % dry sed.)

Figure 12